Separation Science and Technology
Publication details, including instructions for authors and subscription information:
http://www.informaworld.com/smpp/title~content=t713708471

Chromatographic Behavior of a Cholesteryl Myristate Stationary Phase in an Electric Field

R. B. Westerberg[ab]; F. J. Van Lenten[ac]; L. B. Rogers[ac]
[a] DEPARTMENT OF CHEMISTRY, PURDUE UNIVERSITY, WEST LAFAYETTE, INDIANA [b] Jackson Laboratory, Organic Chemicals Department, E. I. du Pont de Nemours & Co., Wilmington, Delaware [c] Chemistry Department, University of Georgia, Athens, Georgia

To cite this Article Westerberg, R. B. , Van Lenten, F. J. and Rogers, L. B.(1975) 'Chromatographic Behavior of a Cholesteryl Myristate Stationary Phase in an Electric Field', Separation Science and Technology, 10: 5, 593 — 616
To link to this Article: DOI: 10.1080/00372367508058042
URL: http://dx.doi.org/10.1080/00372367508058042

SEPARATION SCIENCE, 10(5), pp. 593–616, 1975

Chromatographic Behavior of a Cholesteryl Myristate Stationary Phase in an Electric Field

R. B. WESTERBERG,* F. J. VAN LENTEN,† and L. B. ROGERS†

DEPARTMENT OF CHEMISTRY
PURDUE UNIVERSITY
WEST LAFAYETTE, INDIANA 47907

Abstract

Changes in peak shape which accompany the imposition of an electric field were examined by moments analysis. Although peak maxima shifted significantly, only slight changes were observed in the value of the peak mean. Column efficiencies calculated from the second central moment indicated that the field lowered the resistance to mass transfer, probably as a result of electric field-induced convection of the stationary phase.

INTRODUCTION

The ordered nature of liquid crystals gives rise to many interesting properties which have been discussed in a number of reviews (*1–6*) and books (*7–14*). Liquid crystals have been used as gas chromatographic stationary phases (*12*) for the separation of the structural isomers, particularly the positional isomers of benzene derivatives (*13–21*). The thermodynamic aspects of mesophase-solute interactions have also been studied in gas chromatographic experiments (*22–29*). Chromatographic experiments can be used to indicate the phase transitions that occur in a liquid crystal stationary phase (*30*) and to determine the diffusion coefficients in mesophases (*31*).

*Present address: Jackson Laboratory, Organic Chemicals Department, E. I. du Pont de Nemours & Co., Wilmington, Delaware 19898

†Present address: Chemistry Department, University of Georgia, Athens, Georgia 30602

Since liquid crystalline substances are affected by electric and magnetic fields, speculation arose in the literature that a field could be used to modify the solubility characteristics of liquid crystalline phases (*12*). Subsequently, reports appeared (*32*, *33*) concerning changes in chromatographic behavior that accompanied the imposition of an electric field on a wire in a glass capillary column that had been coated with a liquid crystal phase. There were large changes in the capacity factors, calculated from peak maxima, and in peak shapes, especially the extent of tailing.

The purpose of the present study was to employ moments analysis to examine the effects of an electric field on the gas chromatographic properties of cholesteryl myristate. The object was to differentiate changes in equilibrium values from changes in the dynamic characteristics of the column. Experimentally, the dependences of both the center of gravity and zone spreading on the parameters of linear velovity and column potential were of primary interest. One important aspect of this approach is that the value of the peak maximum and peak mean can substantially differ (*34*); however, the peak mean usually represents the accepted value of the ideal retention time (*34–37*) because the first moment is defined by the equilibrium constant for the distribution of solute between the two phases. The second moment, which depends upon dynamic factors such as rates of mass transfer (*35*, *36*), can be used to calculate column efficiencies. In that way the ambiguity associated with efficiencies calculated for an asymmetric peak on the basis of width at a particular height is also avoided.

There are several aspects of moments analysis that affect the requirements placed on the apparatus, the experimental design, and the interpretation of the data. The most obvious is that, in order for the use of moments analysis to be practical, highly precise data acquisition and use of a computer for data analysis are required. In addition, the signal-to-noise ratio must be high because the higher moments are quite sensitive to error (*35*) introduced by random noise. Finally, the integration limits and the number of data points obtained across a peak can affect the observed accuracy (*36*). The requirement of a finite cutoff in the data can, in some cases, impose a fundamental restraint on the interpretation of the center of gravity (*38–41*) and may affect the observation of non-equilibrium phenomena such as flow-dependent retention volumes (*38*, *41–44*).

The choice of cholesteryl myristate as the stationary phase was based on several considerations. First, cholesteryl myristate has been utilized in previous investigations of charged columns, and has shown resistance to chemical change on borosilicate glass (*33*). Second, Schnur and

Martire have investigated surface effects (*26*) with myristate and found a negligible effect on the thermodynamic properties as determined by gas chromatography. Furthermore, the availability of the thermodynamic data expedites determination of column loading. Finally, cholesteryl myristate has been reported (*45*) not to exhibit a different number of phases on cooling and melting, whereas many other straight-chain cholesteric esters exhibit irreversible phase behavior.

In the present study the main interest was in the region of flow rate where chromatographic behavior was dominated by resistance to mass transfer in the stationary phase. Since this implies a minimal contribution to zone spreading due to longitudinal diffusion, it was decided to use helium as a carrier gas so as to minimize resistance to mass transfer in the gas phase. On a more pragmatic note, the desire to accurately reset to a particular flow rate under conditions of computer control dictated the use of an automatic flow controller for which optimal performance was realized with helium.

EXPERIMENTAL

Reagents

Cholesteryl myristate from Eastman Kodak was used as received. Dicholoromethane (reagent grade, J. T. Baker) and tetrahydrofuran (reagent grade, Mallinckrodt) were used as solvents to make up solutions for coating the capillary columns.

The primary solutes were *n*-pentane, *n*-hexane, cyclopentane (99% mole pure, Phillips Petroleum Co.) and cyclohexane (GC-spectrometric grade, J. T. Baker Co.).

Methane was used as the nonretained solute. The carrier gas was 99.9% pure Airco helium. Airco hydrogen was used for the flame ionization detector. Gases were passed through 4A molecular sieve traps.

Apparatus

All columns were prepared from borosilicate glass and had an internal electrode of 36-gauge chromel-A wire (Hoskins Mfg. Co., Detroit, Michigan). The earlier method of column construction remained unchanged (*33*), except that the process of coating the column with graphite was satisfactorily accomplished by merely dipping the column in graphite paste.

A large multioven chromatograph capable of controlling the temper-

ature to $\pm 0.02^{\circ}C$ was constructed using an insulating refractory fiber board (Maranite, Johns-Manville) and lined on most of the interior surface with a 2.5-cm thick sheet of refractory fiber felt (Type CRF 300 Cerafelt, Johns-Manville). Brisk air circulation was provided by an 18-cm diameter "squirrel cage" fan which was powered by a 1700-rpm electric motor (1/2 hp, Steveco 59600). Oven temperature was maintained by a Thermotrol proportional temperature controller (Hallikainen Instrument Co., Richmond, California) modified to operate in a zero-crossing mode. A platinum Stikon (Rdf Corp., Hudson, New Hampshire) resistance element was used as a temperature sensor.

The oven temperature was measured using a platinum resistance thermometer, model 104T transfer standard (Rosemount Engineering Co., Minneapolis, Minnesota), in conjunction with a Mueller bridge. A resistance bridge with a thermistor bead sensor was used to evaluate the temperature stability of this oven. At $51^{\circ}C$ the temperature was controlled to $\pm 0.015^{\circ}C$ over the short term with a baseline drift of less than $0.01^{\circ}C/hr$. The existence of temperature gradients was investigated by placing the thermistor at eleven widely separated locations in the oven. The largest temperature gradient detected was about $0.08^{\circ}C$. It should be emphasized that the volume probed was many times larger than that actually occupied by the column alone.

Flow control and measurement were provided by a model FCS-100 mass-flow controller (Tylan Corp., Torrance, California). This instrument provided a 0 to 5 V output directly proportional to mass flow rate over the range 0 to 50 sccm. Computer control of flow rate was achieved by providing a set-point voltage from an 11-bit plus sign digital-to-analog converter. Maximum flow rate was specified by a negative 5 V set-point signal while a set-point of 0 V resulted in essentially no flow. Convenient meter indication of flow rate was made using a model LF-50 mass flowmeter (Hasting-Raydist, Inc., Hampton, Virginia) placed downstream from the automatic flow controller.

Column head-pressure measurements were made using a model 538-12 Barocel differential transducer and a 1014-A electronic Manometer (Datametrics, 340 Fordham Road, Wilmington, Massachusetts). A full-scale reading of 1000 Torr resulted in an output of 10 V. The mass-flow devices and the Barocel transducer were mounted in a glass-fronted chamber which was held at approximately $32^{\circ}C$ and, at any one point, to within $\pm 0.1^{\circ}C$ by a zero-crossing triac temperature controller that used a thermistor sensor.

A flame ionization detector (1800 series, Varian Aerograph, Walnut

Creek, California), which had been modified (*46*) to reduce dead volume, was used as the chromatographic detector. The output signal from the electrometer (Varian Aerograph, Model 500 D) was fed into the amplifier system which used two low-drift operational amplifiers (Analog Devices, Model 184 L) before signal transmission. The flame ionization unit was housed in a small chamber which held a cartridge heater placed against the body of the detector. The detector temperature, which was set at 155°C, was determined using an iron–constantan thermocouple with an ice-point reference.

The signals from the flow and pressure devices plus the signal from the flame ionization detector were measured by an auto-ranging multichannel analog-to-digital converter (Anscan, Model 3700, Beckman Instruments, Fullerton, California).

Computer control over the electrode voltage source (Beckman, Duostat Regulated Power Supply) and the various gas sampling and switching valves made use of an experimental interface which has been described previously (*47*). In brief, the experimental interface was used to turn on zero-crossing solid-state relays and line voltage to a device in response to computer command. Several 4-port, two-way solenoid valves (Air-switch, Model 3C301, Mosier Industries Inc., Dayton, Ohio) were used to actuate pneumatically the sampling and switching valves.

An exponential dilution flask was fabricated in the glass shop from two borosilicate glass spherical O-ring joints (size 75/50, 57 mm o.d.). The flask was sealed at the joint using the specified size 75 ball-and-socket type clamp and a size 2-229 Viton O-ring. This particular design was more immune to breakage from clamping stresses than a similar earlier model which featured a ground-glass seal (*48*).

Procedures

Three columns were prepared using two different solvents to make up the coating solution (*33*). All columns were then conditioned at 100 to 120°C with nitrogen flowing through the columns. Some characteristics of these columns are given in Table 1.

The columns were plumbed into the system using shrinkable Teflon tubing. It was found that the occurrence of leaks could be minimized at the point where the electrode was fed between the glass capillary and shrinkable tubing by sealing the connection using a high-temperature epoxy. Columns were mounted directly over the oven fan.

Flow rate through the sampling system was controlled using a differ-

TABLE 1

Coating Procedures and Characteristics of Capillary Columns

Column	Coating solution (w/v%)	Plug flow (cm/sec)	Radius (mm)	Film thickness (μm)	Length (cm)
1	50(CH_2Cl_2)	2	0.25	2.31	3560
2	50(CH_2Cl_2)	2	0.24	2.29	2780
3	20(THF)	3	0.23	1.64	2600

ential flow controller. The rest of the sampling system consisted of an exponential dilution flask which could be charged with either methane, for a nonretained peak, or solute vapors through the action of one of two computer-controlled air-actuated valves. The actual injection onto the column was accomplished by sampling the effluent from the dilution flask with a Seiscor gas-sampling valve. Methane was contained in a 1-liter pressurized reservoir, and was introduced into the dilution flask by opening a valve for 1 to 2 sec. Samples of solute vapors were obtained by using a switching valve to pass the helium stream through a two-stage saturator and into the dilution flask for a constant period of 8 sec. Sample size was controlled by changing the length of time between charging up the dilution flask and sampling the effluent from the flask.

The overall experiment featured computer-automated isothermal chromatographic experiments at a number of different flow rates. After the electronic flow controller had set the flow rate, the column-head pressure was required to stabilize to $\pm 0.1\%$ for a 30-sec interval. Then a sample of methane was injected so as to determine the residence time of a nonretained species. Experiments with retained solutes on the uncharged and charged columns followed. At the termination of each experiment the digitized chromatogram, the values of head pressure and the mass flow rate, and the results of calculations were stored on magnetic tape.

The chromatographic efficiency observed was reproducible with duplicate experiments performed sequentially. However, resetting conditions with a change in the flow rate could yield a somewhat different average value for efficiency. For that reason the efficiency values were taken as the average of a minimum of four values with at least one resetting of the flow rate. It was found that reduplicating the same series of experiments in the same order of flow rates gave closely comparable results even after a reset of the experimental conditions following a change in column temperature.

The peaks in this study were asymmetric, and many of them were

severely tailed. Accurate work requires that all of the tail be included in the calculation (*36*). As a result, more data were acquired after the peak maximum than before. Criteria were set for data intervals in terms of the standard deviation of a peak calculated on the basis of the second moment. Data were acquired for a minimum of approximately one and one-half standard deviations before the peak maximum, and seven following the maximum. Since the peaks were asymmetric, the standard deviation was much larger than predicted from the front half of the peak. As a result, the criterion for placement of the integration limit before the peak maximum appears to be much closer to the front of the peak than is actually the case. A total of 230 points were acquired for each peak, using data intervals that ranged from 0.2 to 2.5 sec/pt.

Calculations

Due to the presence of the internal electrode, the typical means of visually measuring the radius using a magnifying glass with a calibrated grid was checked in another way. The effective radius was calculated from the pressure drop measured across the capillary under particular conditions of temperature and flow rate. This approach was also useful because the column radius might have experienced variations during the drawing process, and the pressure drop reflected the average value of the radius. Specifically, from the equations presented by Ettre (*49*), the following relationship was determined:

$$r = \sqrt{8\eta\bar{\mu}L/\Delta p} \tag{1}$$

where r is the column radius, η is the viscosity of the gas, L is the length of the column, Δp is the pressure drop, and $\bar{\mu}$ is the average linear velocity. The radii calculated on the basis of pressure drop were approximately 10% lower than those visually measured at each end of the capillary.

An apparent film thickness for stationary phase was calculated from the relationship (*50*)

$$d_f = 273rk/2T\rho_T V_g \tag{2}$$

where V_g is the specific retention volume, T is the column temperature, k is the capacity ratio, and ρ_T is the density of the stationary phase. The specific retention volume was taken from the data of Martire et al. (*23*) for hexane at 86°C. The density for cholesteryl myristate was estimated on the basis of that given for cholesteryl palmitate (*51*).

The zeroth through the second moments were computed using the

appropriate summations. The second central moment was calculated by adjusting the second moment with the value of the first moment.

The capacity ratio was calculated both on the basis of retention time at the center gravity, t_c, and on the basis of retention time at peak maximum, t_m. The retention time at peak maximum was found on the basis of the inflection point of a second degree polynomial which was fit to seven points across the top of the peak using Gram polynomials (*52*). The capacity ratio based on retention time at peak maximum is given by

$$k_m = (t_m - t_o)/t_o \tag{3}$$

where k_m is the capacity ratio based on peak maximum, and t_o is the retention time at the center of gravity for the nonretained methane peak. The capacity ratio based on retention time at the center of gravity was calculated in an analogous fashion with the substitution of t_c for t_m. (Any unsubscripted citation of the capacity ratio should be assumed to represent a value calculated on the basis of the center of gravity.) For a replicate experiment that was run 1 week later with the reset of all experimental conditions, the averaged values of k_c for a charged column agreed to 0.03%. For the uncharged column, agreement was a more representative 0.48%.

A normalized difference between the "ideal" retention time, t_c, and retention time at peak maximum was calculated by

$$t_D = (t_c - t_m)/t_c \tag{4}$$

where t_D represents the difference between the two retention times normalized by the retention time at the center of gravity.

The average linear velocity of the carrier gas was calculated on the basis of the retention time of a nonretained peak by

$$\bar{\mu} = L/t_o \tag{5}$$

Using this method, the flow rate was typically determined with an average relative standard deviation of 0.2%. This value includes the effect of at least one reset of the flow rate.

Column efficiency was calculated from the second central moment by

$$H = \sigma^2 L/t_c^2 \tag{6}$$

where H is the height equivalent to a theoretical plate and σ^2 is the second central moment.

Coefficients of resistance to mass transfer in the liquid phase, C_l, were

calculated in a manner similar to Grushka and Solsky's treatment of capillary column data (*31*). This involves subtracting the contributions of the B term and C_g term from the observed HETP value. The remaining contribution to peak spreading is assumed to result from resistance to mass transfer in the stationary phase. The Fuller, Schettler, and Giddings equation (*53*) was used to calculate diffusivities of the solutes in the gas phase.

The dependence of the C_l term on the parameters of film thickness, d_f, diffusion coefficient in the stationary phase, D_l, and capacity ratio, k, is given by the following relationship:

$$C_l = 2kd_f^2/3(k+1)^2D_l \tag{7}$$

To facilitate comparisons of mass-transfer characteristics between solutes of differing capacity ratios, the values of C_l were normalized by dividing the term by $k/(k+1)^2$.

Chromatograms were plotted using an abcissa of eluted volume instead of time. The eluted volume was calculated using the product of the elapsed time, the average linear velocity, and the cross-sectional area of the capillary. The advantage of this approach was that it allowed a direct comparison of the shapes of two chromatograms acquired at different values of linear flow. As a result, the peak shapes reflected only the dependence of the chromatographic process on flow rate and did not depend upon the rate of digitization.

RESULTS

Effect on Retention Behavior of Column Potential and Flow Rate

The capacity ratio, k_c, calculated on the basis of the peak center of gravity should be insensitive to peak shape changes and reflect changes in actual retention behavior. Table 2 shows that only small changes in k_c occurred as a function of both flow and potential. However, a small, but systematic, trend toward larger values of k_c was observed at lower values of flow on both the charged and uncharged column. In contrast, the capacity factor calculated from the retention time at the peak maximum (k_m) exhibited a strong dependency on both flow rate and column potential, in agreement with earlier work (*32*, *33*). Furthermore, the difference between the retention time at the center of gravity, t_c, and at the peak maximum, t_m, is seen to be a function of flow rate. As the flow rate de-

TABLE 2

Effect of Applied Potential on k_c and k_m and on the Normalized Difference between the Mean and the Maximum of a Peak as a Function of Flow Rate Using *n*-Pentane at 80.9°C

Av linear velocity (cm/sec)	500 V			0 V				
	k_c	k_m	t_D	k_c	k_m	t_D	$\%\Delta k_c$	$\%\Delta k_m$
73.3	0.2929	0.182	0.0855	0.2859	0.106	0.136	2.4	41.5
67.6	0.2961	0.191	0.0816	0.2909	0.109	0.139	1.9	42.9
61.5	0.2963	0.197	0.0766	0.2926	0.118	0.137	1.2	39.9
55.2	0.2970	0.204	0.0708	0.2960	0.122	0.133	0.2	40.4
48.7	0.2988	0.216	0.0642	0.2988	0.134	0.126	0.0	38.0
41.8	0.2994	0.226	0.0569	0.287	0.144	0.119	0.2	36.3
34.5	0.2994	0.237	0.0480	0.3013	0.156	0.112	−0.8	34.2

creased, the retention time at the peak maximum approached the center of gravity. This behavior is shown in Table 2 where the normalized difference between t_c and t_m is tabulated against linear velocity.

The independence of k_c and the dependence of k_m on potential was a general phenomenon. A typical pair of chromatograms is shown in Fig. 1, and typical data for different solutes at two temperatures are shown in Table 3. Because, as seen in Table 2, k_m exhibited a dependence on both column potential and flow rate, the k_m data in Table 3 were taken at identical linear flow rates.

TABLE 3

Behavior on Column 1 of k_c and k_m with Applied Potential for Four Solutes at Two Temperatures[a]

Temp (°C)	Solute	k_c		Difference (%)	k_m		Difference (%)
		500 V	0 V		500 V	0 V	
80.9	*n*-Pentane	0.297	0.294	1.01	0.214	0.134	37.3
	n-Hexane	0.591	0.588	0.57	0.486	0.301	38.1
	Cyclopentane	0.684	0.681	0.44	0.566	0.403	28.7
	Cyclohexane	1.325	1.323	0.02	1.190	0.847	28.8
86.0	*n*-Pentane	0.259	0.258	0.39	0.188	0.121	35.6
	n-Hexane	0.606	0.605	0.17	0.423	0.259	38.7
	Cyclopentane	[b]	[b]	[b]	0.524	0.367	29.9
	Cyclohexane	1.149	1.143	0.52	1.033	0.700	32.2

[a]Value at 48 cm/sec.
[b]No data.

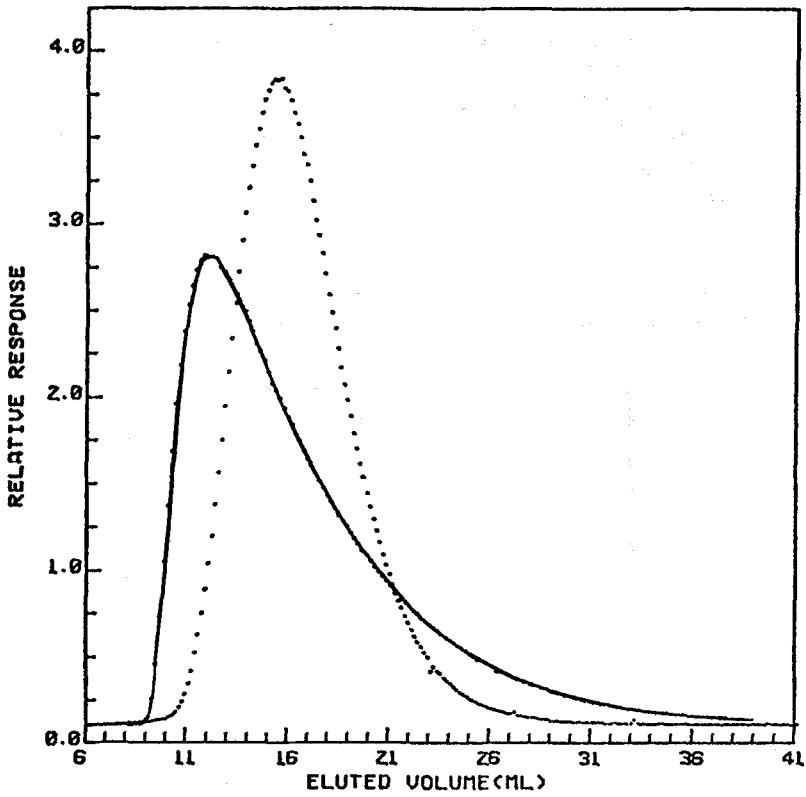

FIG. 1. Effect of potential on peak shape for cyclohexane at an average linear velocity of 61.7 cm/sec: (· ·) 500 volts and (—) 0 volts.

It was also observed that a reduction in carrier gas flow rate affected the peak shape in a manner similar to potential. Either a reduction in flow rate or imposition of potential led to a more nearly symmetrical peak that had a greater retention volume measured at the peak maximum. The similarity between the effects of flow rate and potential is dealt with in further detail in the following section.

Column Efficiency

The changes in peak shape produced by the electric field were accompanied by increases in chromatographic efficiency. As shown in Fig. 2, this behavior was reflected in the observation of two distinct van Deemter

curves for the charged and uncharged columns. The observed efficiencies were found to depend slightly upon previous flow history. Hence the flow rates for a van Deemter were studied in a random order so as to average out those effects. The validity of the values for the efficiencies was tested by replicating a series of experiments after resetting all experimental conditions. As may be seen in Table 4, the uncertainty in replicating the data was no greater than the uncertainty associated with the original determinations.

On the basis of the van Deemter data, imposition of a potential lowered the resistance to mass transfer. The magnitude of the change in mass

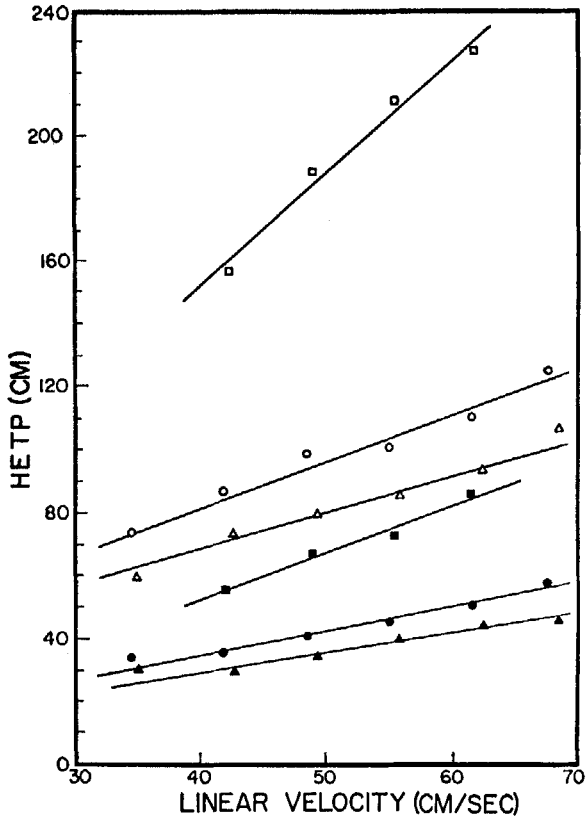

FIG. 2. Effect of an electric field on column efficiencies: (□) cyclopentane at 81 °C, (○) pentane at 81 °C, and (△) pentane at 88 °C. Solid symbols: 500 volts. Open symbols: 0 volts.

TABLE 4

Reproducibilities on Column 1 of HETP Values for *n*-Pentane at 80.9°C

Av linear velocity (cm)	500 V			0 V		
	Av_1 HETP (cm)	Std dev (%)	$Av_1 - Av_2$ (%)	Av_1 HETP (cm)	Std dev (%)	$Av_1 - Av_2$ (%)
67.6	58.1	3.4	−4.1	125.6	6.4	−5.4
61.5	51.1	2.8	−7.8	115.9	7.2	+0.4
55.2	46.2	1.4	−8.8	113.8	3.9	+1.6
48.7	41.3	3.8	−7.2	99.2	4.4	−1.2
41.8	35.9	1.0	−5.0	87.1	2.3	+0.3
34.5	34.0	2.9	+0.6	74.2	5.3	−2.5

TABLE 5

Normalized C_1 Terms for Four Solutes as a Function of the Temperature of the Stationary Phase

Solute	Temp (°C)	Column 1		Column 2		Column 3	
		500 V	0 V	500 V	0 V	500 V	0 V
n-Pentane	80.9[a]	4.72	11.4	4.68	9.48	4.68	7.83
n-Hexane		5.43	12.8	5.43	11.70	5.12	8.76
Cyclopentane		5.93	16.6	—	—	—	—
Cyclohexane		7.29	22.7	—	—	—	—
n-Pentane	86.0[b]	4.11	10.1	3.43	8.04	3.85	7.71
n-Hexane		4.14	11.7	4.10	10.20	4.10	8.55
Cyclopentane		4.89	12.7	—	—	4.62	8.76
Cyclohexane		6.30	19.1	4.92	14.10	—	—
n-Pentane	93.0[c]	2.90	7.6	2.54	6.55	2.92	6.09
n-Hexane		4.51	14.3	3.40	10.30	3.11	6.59

[a]Mesophase (*23*).
[b]Barely into the isotropic phase (*23*).
[c]Isotropic phase.

transfer coefficients is indicated in Table 5. The original values have been divided by the quantity $k/(k+1)^2$ so as to eliminate differences in resistance to mass transfer that arose because of differences in capacity ratios. Note that the values of the normalized C_l terms appeared to agree better from column to column when the column was charged. Note also that the relative change in the resistance to mass transfer did not rise above a factor of 4 and that the magnitude of change with potential seemed independent of the solute. Furthermore, since the normalized C_l term is inversely proportional to the diffusion coefficient in the stationary phase, the relative magnitudes of these terms can be predicted from the Wilke-Chang equation (*54*) for liquid diffusion coefficients. Qualitatively, the correct trend is seen for pentane vs hexane, and cyclopentane vs cyclohexane. Namely, the smaller molecule exhibits the lower resistance to mass transfer. In general, the columns exhibited dominance of mass transfer in the stationary phase to such an extent that the B term and C_l term corrections were very small. The C_l term could be approximated to within 1 % merely by dividing the efficiency by the average linear velocity.

The similarity between the effects of charging the column and reducing the carrier gas flow rate was investigated further on the basis of the observed values of column efficiency. Due to the dominance of the chromatographic process by resistance to mass transfer, peaks that exhibited similar efficiencies should also be characterized by a similar value of C_l. If the major effect of charging the column was to lower the C_l term, then peak shape from a charged column should be quite similar to one from an uncharged column, provided that conditions were such that both exhibited equivalent chromatographic efficiencies. In order to normalize to the same chromatographic efficiency, two chromatograms were acquired at different values of linear velocity. It was possible to reduce the linear velocity on the uncharged column so that virtually the same number of plates were generated without potential as were generated on the charged column at the greater linear flow rate. Such an example is shown in Fig. 3. Note the striking similarities of the peak shapes.

In order to estimate the effect of the wire, the efficiency of the inert peak was determined. Since the spreading of an inert peak should result mainly from longitudinal diffusion, any additional spreading was assumed to be a result of the wire. Determination of a longitudinal diffusion term yielded a calculated value for efficiency that was better than observed. When the difference between the calculated and experimental values for efficiency was determined, an apparent eddy-diffusion term of 0.28 cm for column 1 and 0.43 for column 2 was obtained. It would appear that

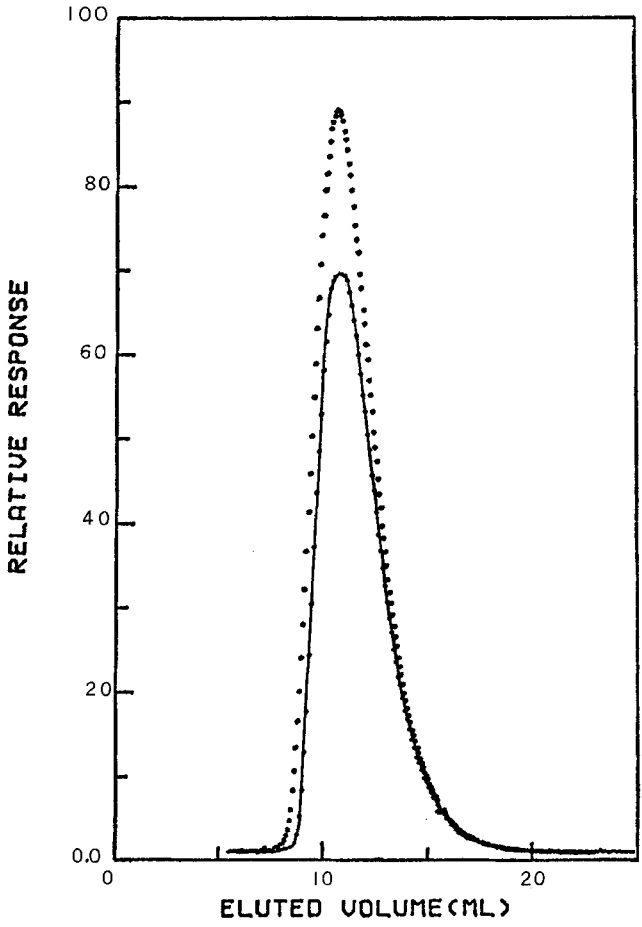

FIG. 3. Comparison of peak shapes for *n*-pentane at 80.9 °C on a charged and uncharged column having nearly the same value of column efficiency. (··) Charged column, average linear velocity of 55.4 cm/sec and HETP of 76.9 cm. (—) Uncharged column, average linear velocity of 15.7 cm/sec and HETP of 76.6 cm.

this zone spreading is caused by flow inequalities about the wire and also about droplets of stationary phase bridging between the wire and the capillary wall.

The effect of potential on efficiency was manifested in both the supercooled liquid and in the liquid at temperatures well above the isotropic point. Figure 4 depicts the dependence of resistance to mass transfer, as approximated by dividing HETP by $\bar{u}$, of both the charged and uncharged column as a function of temperature. An increase in the rate of diffusion of the solute probably was the main factor that caused the steady downward trend of C_l values seen in Fig. 4. It is also interesting to note that the difference between the heating cycle and cooling cycle was very small until about 80°C where a hysterisis effect is seen in the capacity-ratio curve and in both C_l curves.

Even in some additional experiments run at a temperature of 127°C, typical changes in efficiency with potential were observed. Hence, the liquid-crystalline state per se may not be the basis for observed effect of potential.

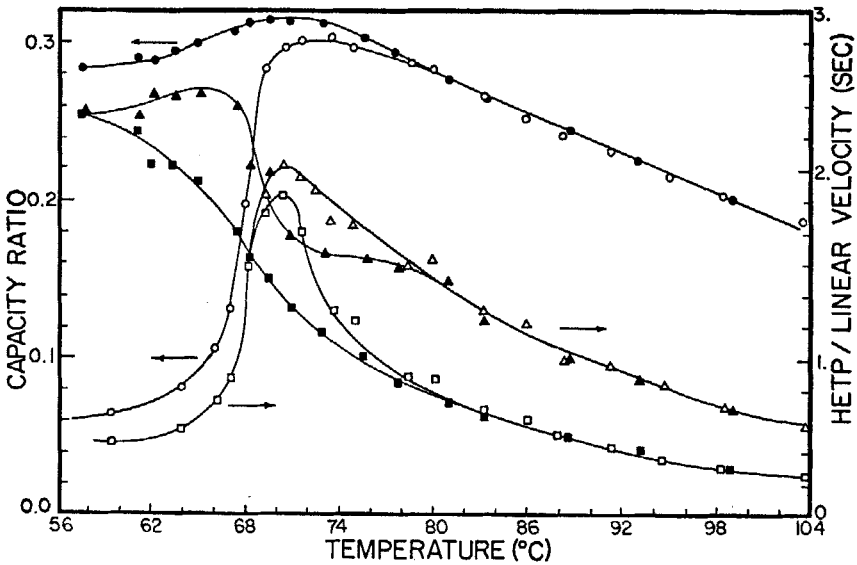

FIG. 4. Changes in capacity ratio and mass-transfer coefficient for *n*-pentane as as a function of temperature: (○) Capacity ratio, (△) HETP/μ at 0 volts, and (□) HETP/μ at 500 volts. Solid symbols: cooling cycle. Open symbols: heating cycle.

Effect of Sample Size

No change in chromatographic properties with sample size was observed on the uncharged column over a range of sample sizes of greater than one order of magnitude. However, in the course of these experiments it became apparent that the peak observed on the charged column was asymmetrically broadened at the leading edge of its base. Injection of samples about a factor of 10 smaller than those normally used revealed that the size of the broadening was disproportionately greater at smaller sample size. An area-normalized plot for two different sizes of samples is shown in Fig. 5. It is apparent that the smaller sample exhibited the

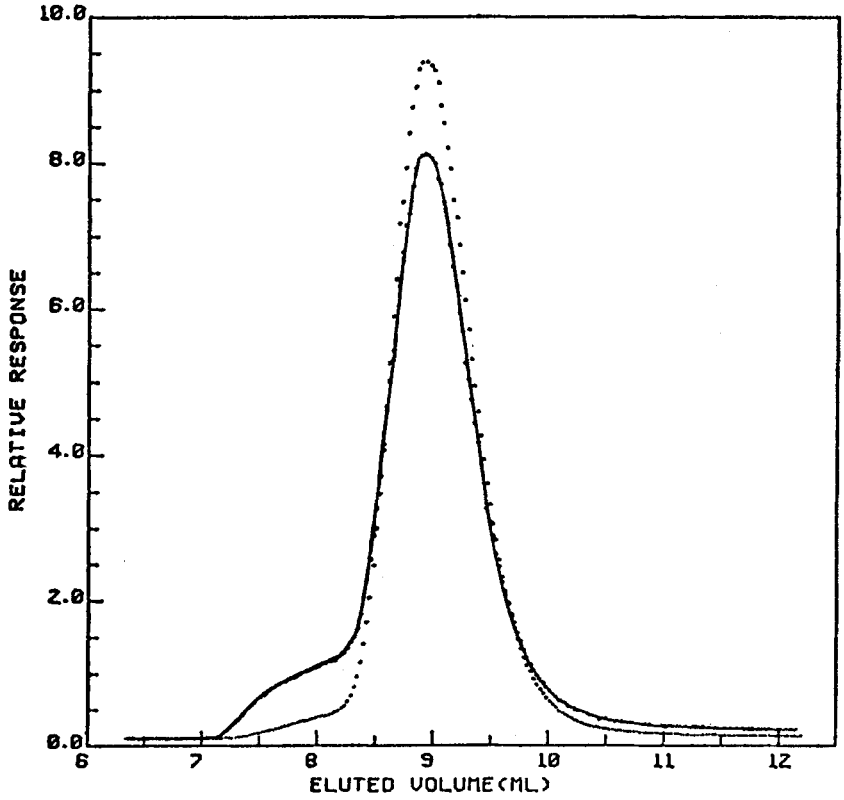

FIG. 5. Effect of an 8.8-fold increase (··) in sample size on the shape of area-normalized peaks for *n*-pentane at 80.9 °C and average carrier gas velocity of 10 cm/sec: (··) larger sample and (—) Smaller sample.

greater amount of fronting. However, when considered with respect to their true sizes, the absolute magnitude of the effect was greater for the larger sample.

This asymmetric broadening was observed for all solutes and at both high and low flow rates. The possibility of a displacement of residual chlorinated solvent was checked by coating a column with a solution made up with tetrahydrofuran as the solvent. However, that column exhibited the same behavior.

DISCUSSION

The invariance of the center of gravity with the imposition of a potential and the existence of separate van Deemter curves for charged and uncharged columns indicate that the potential acts to alter the mass transfer in the liquid phase with little or no effect on the thermodynamic interaction between the solute and stationary phase. The effect of potential on peak shape must be intimately related to the very inefficient behavior of the columns which caused a large departure from ideal behavior. Clearly, an applied potential lowered the resistance to mass transfer and more plates were generated. The increased efficiency was reflected in a closer approach to ideal chromatographic behavior and a shift of the peak maximum toward the center of gravity. The effect of decreasing the flow rate was similar to that of applying a potential because the lower flow rate merely served to decrease the resistance to mass transfer and to promote a closer approach to ideal behavior.

One critical aspect of this discussion has been that poor chromatographic efficiency can give rise to peak distortion. The theoretical developments presented by Rony and Funk (*39*, *40*) and Wicăr et al. (*41*) are critical in this regard and, in addition, provide insight into the observed flow-dependent capacity ratios.

Taking first the topic of changes in retention volumes, both sets of authors discussed the idea that, under real conditions, one would expect the first moment to depend upon mass transfer characteristics in instances where resistance to mass transfer was quite high. Furthermore, Rony and Funk (*40*) indicated that mean retention of a peak will vary between that of a nonretained peak and the retention time dictated by the capacity ratio depending on the quality ϕ which reflects the ratio of the "rate of diffusional mass transfer in the liquid film to the corrective gas-phase mass transfer in the axial direction." They showed that low values of ϕ can reduce the mean retention time.

We observed greater values of the capacity ratio at lower values of flow. Hence lowering the flow rate reduced the resistance to mass transfer and increased the value of Rony and Funk's ϕ. Thus our observations concerning the capacity ratio are in accordance with their predictions, and the small differences between the capacity ratio on the charged and uncharged column probably reflect the difference in C_l between the two columns.

Second, both sets of authors addressed themselves to the relationship between nonideal behavior and peak distortion. Wicăr et al. (*41*) showed that the difference between the ideal retention time and the retention time at peak maxima, after being normalized by the ideal retention time [similar to the $(t_C - t_m)/t_C$ we used], exhibited a linear dependence on the term $\Sigma C/t_o$, where ΣC represents the summation of the gas and liquid resistance to mass transfer terms. Since, in the case of our data, $H/\bar{\mu}$ was approximately equal to ΣC, their relationship may be interpreted as indicating that the difference between the ideal retention time and that observed at peak maximum decreases as the number of plates were increased. If we accept the value of t_C as good approximation of the ideal retention time, Table 2 shows that our data followed the predicted trend. Rony and Funk (*38*, *39*) showed peak distortion as a function of their ϕ term. Since ϕ is given by

$$\phi = (8D_l k/3\bar{\mu})/(\bar{\mu}/r) \tag{8}$$

we see that either a change in the linear velocity or in the effective diffusion coefficient can influence the peak shape. That is, either slower velocities or a greater D_l can lead to more nearly symmetrical peaks.

Both of these treatments predict peak distortion only in the limit of large resistances to mass transfer. The inefficient columns we used displayed values of $\Sigma C/t_o$ that were roughly an order of magnitude greater than presented by Wicăr (*41*). Accordingly, the overall resistance to mass transfer was well within the range for which peak asymmetry would be expected. Thus, in terms of the overall evidence, it appears reasonable to account for changes in peak shape solely on the basis of changes in column efficiency (i.e., changes in the $C_l\bar{\mu}$ term).

It is worthwhile to examine the characteristics of columns that exhibited effects with applied potential. First, the extremely high resistance to mass transfer was greater than would have been expected from values calculated using the apparent film thickness. It is obvious that the film was not uniformly coated over the surface of the capillary, but rather was in the form of many tiny droplets or puddles at the contact points between the wire and the glass. The resulting geometric factor

produced an extremely high C_l term. However, the lower efficiency and the fact that mass transfer in the liquid phase was the dominant source of zone spreading make any change in the C_l term quite dramatic.

Second, when lower liquid loadings were used, previous workers (*32*) reported that potential effects were less dramatic or even nonexistent. We also found the same type of behavior at lower liquid loadings, and furthermore it was easily observed visually that such columns gave narrower peaks than did columns which exhibited an effect with potential. Also, of the three columns studied, column 3, which had the lowest loading of stationary phase, exhibited the smallest changes in the normalized C_l term with imposition of a potential as may be seen in Table 5.

There are two factors that might account for such behavior. First, at lower liquid loadings the efficiency of a column will be higher and the effect of nonideality will be relatively smaller. Second, the apparent eddy-diffusion term will dominate the sources of zone spreading so that any effect due to changes in resistance to mass transfer will be small compared to the other sources of zone spreading. In other words, the low efficiency and the dominance of the C_l term, which causes the inefficient behavior, will make a three- or fourfold change in C_l quite dramatic. If such a change in C_l were to occur on a much more efficient but mass-transfer-limited column, a somewhat different behavior would be observed. Since the chromatographic processes would be much closer to ideality, a shift of the peak maximum would not be observed. A decrease in zone spreading should still occur, but it might be so small on a relative basis as to be imperceptible.

The existence of droplets and/or puddles could also explain our observation that column efficiencies were somewhat dependent upon the history of the flow rate. Changes in the flow rate could lead to a redistribution of the liquid phase and yield a somewhat different efficiency as a result of a new film geometry.

There are two phenomena described in the liquid crystal literature which could be involved in an electric field-induced change in C_l. The first phenomenon involves anisotropic diffusion coefficients which depend on the direction of liquid crystal orientation (*55*). If anisotropic diffusion were at play, a change in efficiency could occur because the field-induced change in the stationary phase would result in an orientation that exhibited a greater diffusion coefficient. However, the change in peak shape on the charged column was also observed for a column that had been held at approximately 45°C above the isotropic transition temperature for 30 min before the *n*-pentane was injected. Thus, unless ordering caused by a

wall effect was at play, the prospect of anisotropic diffusion appears to be unlikely.

The second phenomenon relates to the observation that, under the proper conditions, an electric field can induce flow in a mesophase. This phenomenon can produce regular domain patterns (*6*) which exhibit vortex motion (*56*) or may produce a state of random turbulence which is referred to as dynamic scattering (*57*). Since both processes involve physical motion of the liquid, either could lower C_l by contributing to convective mass transport of the solute. Such effects are known to occur with cholesteric and smectic mesophases as well as nematic materials (*58*). Furthermore, in dc fields, induced turbulent flow can occur (*59*) in isotropic liquids. The range of potentials required is reported (*60*) to extend from a "high range" of 150 kV/cm to the "moderate range" of 1.3 to 2.6 kV/cm. As shown below, our use of 500 V over less than 0.3 mm was well within the latter range.

There are several features of the experiments with charged columns that agree with the characteristics of electric field-induced flow of the stationary phase. A contribution to the mass transfer with no effect on the thermodynamics of the solute–solvent interaction is consistent with an enhancement of the mass-transfer process through convective movement of the solvent. The observation of changes in peak shape well above the isotropic point requires that underlying phenomena be present in the isotropic liquid, which is the case with electrohydrodynamic effects. Furthermore, the frequency dependence of the behavior of charged columns is qualitatively similar to that observed for dynamic scattering. For example, dynamic scattering has been observed (*57*, *59*) in a dc or low frequency ac field, but not at higher frequencies. Taylor et al. (*32*) demonstrated that, at higher frequencies, there was no observable effect of potential on chromatographic behavior. The field strength employed in that series of experiments was approximately 20 kV/cm and was within the range over which the electrohydrodynamic phenomena are observed (500 V over a 0.25-mm radius implicitly corrected for the 0.064-mm radius of the wire by calculating the capillary radius from pneumatic data).

Mention should also be made of the possibility of the decrease in resistance to mass transfer with potential arising from a decrease in the effective film thickness or from a change in the stationary phase geometry. If the result of an electrohydrodynamic effect is the spreading out of droplets of the stationary phase, then the change in film geometry will be reflected in the observed efficiency. However, at a fixed flow rate the observed change in efficiency with potential was both reproducible and

reversible. Although it is not conclusive evidence, this fact does not tend to make the picture of physical rearrangement of the stationary phase a particularly attractive hypothesis.

There are two tentative rationalizations which we believe can be ruled out as possible explanations for the assymetric broadening of a peak on its leading edge. First, displacement of coating solvent entrained within the stationary phase was ruled out by using two dissimilar solvents and finding the same "fronting" effect for each column. Second, breakdown of the solute and/or statioary phase under the influence of the electric field might produce a more volatile species. However, the peak distortion was examined for pentane and cyclohexane, and it seems unlikely that volatile species would be produced in two different cases in such a manner to produce the same type of peak distortion in each case. Examination of the front in this system using mass spectrometry would provide conclusive evidence on this point.

Acknowledgments

Supported in part by the U.S. Atomic Energy Commission under contracts AT(11–1)–1222 and AT(38–1)–854.

Helpful discussions with John Nieman and Edward M. Barrall, both of IBM Corporation, are gratefully noted.

REFERENCES

1. G. H. Brown and W. G. Shaw, *Chem. Rev.*, *57*, 1049 (1957).
2. G. H. Brown, J. W. Doane, and V. D. Neff, *Crit. Rev. Solid State Sci.*, *1*, 303 (1970).
3. S. E. B. Petrie, H. K. Bucher, R. T. Klingbiel, and P. I. Rose, *Eastman Organic Chemical Bulletin, Kodak Publication No. JJ-60-731*, *45*(2), 1 (1973).
4. G. H. Brown, J. W. Doane, and V. D. Neff, *A Review of the Structure and Physical Properties of Liquid Crystals*, C. R. C., Cleveland, Ohio, 1971.
5. A. Saupe, *Angew. Chem. Int. Ed. Engl.*, *7*, 97 (1968).
6. A. Saupe, in *Annual Review of Physical Chemistry*, Vol. 24 (H. Eyring, ed.), Annual Reviews, Palo Alto, California, 1973, pp. 441-71.
7. G. W. Gray, *Molecular Structure and the Properties of Liquid Crystals*, Academic, London, 1962.
8. R. S. Porter and J. F. Johnson, eds., *Liquid Crystals and Ordered Fluids*, Plenum, New York, 1970.
9. G. H. Brown, M. M. Labes, and G. J. Dienes, eds., *Liquid Crystals*, Gordon and Breach, New York, 1966.
10. G. H. Brown and M. M. Labes, eds., *Liquid Crystals 2*, Vols. 1 and 2, Gordon and Breach, New York, 1969.

11. G. H. Brown and M. M. Labes, eds., *Liquid Crystals 3*, Vols. 1 and 2, Gordon and Breach, New York, 1972.
12. H. Kelker and E. Von Schivizhoffen, *Adv. Chromatogr.*, *6*, 247–297 (1969).
13. M. J. S. Dewar and J. P. Schroeder, *J. Org. Chem.*, *30*, 3485 (1965).
14. M. J. S. Dewar and J. P. Schroeder, *J. Amer. Chem. Soc.*, *86*, 5235 (1964).
15. M. J. S. Dewar, J. P. Schroeder, and D. C. Schroeder, *J. Org. Chem.*, *32*, 1692 (1967).
16. H. Kelker, B. Scheurke, and W. Winterscheidt, *Anal. Chim. Acta*, *38*, 17 (1967).
17. J. P. Schroeder, D. C. Schroeder, and M. Katiskas, in *Liquid Crystals and Ordered Fluids* (J. F. Johnson and R. S. Porter, eds.), Plenum, New York, 1970, pp. 169–180.
18. P. J. Poraro and P. Shubick, *J. Chromatogr. Sci.*, *9*, 690 (1971).
19. M. A. Andrews, D. C. Schroeder, and J. P. Schroeder, *J. Chromatogr.*, *71*, 233 (1972).
20. W. Zielinski, D. H. Freeman, D. E. Martire, and L. C. Chow, *Anal. Chem.*, *42*, 176 (1970).
21. A. B. Richmond, *J. Chromatogr. Sci.*, *9*, 571 (1971).
22. H. Kelker and A. Verhelst, *Ibid.*, *7*, 79 (1969).
23. D. E. Martire, P. A. Blasco, P. F. Carone, L. C. Chow, and H. Vicini, *J. Phys. Chem.*, *72*, 3489 (1968).
24. L. C. Chow and D. E. Martire, *Ibid*, *73*, 1127 (1969).
25. L. C. Chow and D. E. Martire, *Ibid.*, *75*, 2005 (1971).
26. J. M. Schnur and D. E. Martire, *Anal. Chem.*, *43*, 1201 (1971).
27. L. C. Chow and D. E. Martire, *Mol. Cryst. Liq. Cryst.*, *14*, 293 (1971).
28. D. G. Willey and D. E. Martire, *Ibid.*, *18*, 55 (1972).
29. D. G. Willey and G. H. Brown, *J. Phys. Chem.*, *76*, 99 (1972).
30. E. M. Barrell, R. S. Porter, and J. F. Johnson, *J. Chromatogr.*, *21*, 392 (1966).
31. E. Grushka and J. F. Solsky, *Anal. Chem.*, *45*, 1836 (1973).
32. P. J. Taylor, R. A. Culp, C. H. Lochmuller, and L. B. Rogers, *Separ. Sci.*, *6*, 841 (1971).
33. P. J. Taylor, A. O. Ntukogu, S. S. Metcalf, and L. B. Rogers, *Ibid.*, *8*, 245 (1973).
34. Kuang-Pang Li, D. L. Duewer, and R. S. Juvet, *Anal. Chem.*, *46*, 1209 (1974).
35. O. Grubner, *Adv. Chromatogr. 6*, 173 (1968).
36. S. N. Chesler and S. P. Cram, *Anal. Chem.*, *43*, 1922 (1971).
37. E. Kučera, *J. Chromatogr.*, *19*, 237 (1965).
38. J. E. Funk and P. R. Rony, *Separ. Sci.*, *6*, 365 (1971).
39. P. R. Rony and J. E. Funk, *Ibid.*, *6*, 383 (1971).
40. P. R. Rony and J. E. Funk, *J. Chromatogr. Sci.*, *9*, 215 (1971).
41. S. Wičar, J. Novak, and N. Ruseva-Rakshieva, *Anal. Chem.*, *43*, 1945 (1971).
42. J. E. Oberholtzer and L. B. Rogers, *Ibid.*, *41*, 1590 (1969).
43. A. K. Moreland and L. B. Rogers, *Separ. Sci.*, *6*, 1 (1971).
44. H. W. Habgood and W. R. MacDonald, *Anal. Chem.*, *42*, 543 (1970).
45. E. M. Barrell, R. S. Porter, and J. F. Johnson, *Mol. Cryst. Liq. Cryst.*, *3*, 103 (1967).
46. R. S. Swingle and L. B. Rogers, *Anal. Chem.*, *43*, 810 (1971).
47. J. E. Davis and E. D. Schmidlin, *Chem. Inst.*, *4*, 169 (1973).
48. L. J. Lorenz, R. A. Culp, and R. T. Dixon, *Anal. Chem.*, *42*, 119 (1970).
49. L. S. Ettre, *Open Tubular Columns in Gas Chromatography*, Plenum, New York, 1965, pp. 38–40.
50. K. D. Bartle, *Anal. Chem.*, *45*, 1831 (1973).
51. R. S. Porter and J. F. Johnson, *J. Appl. Phys.*, *34*, 55 (1963).
52. H. T. Davis, *Tables of the Mathematical Functions*, Vol. 2, Principia, San Antonio, Texas, 1963, pp. 307–308.
53. E. N. Fuller, D. C. Schettler, and J. C. Giddings, *Ind. Eng. Chem.*, *58*, 19 (1966).

54. J. C. Giddings, *Dynamics of Chromatography. Part I. Principles and Theory*, Dekker, New York, 1965, p. 233.
55. W. Franklin, *Mol. Cryst. Liq. Cryst.*, *14*, 227 (1971).
56. P. A. Penz, *Phys. Rev. Lett.*, *24*, 1405 (1970).
57. G. H. Heimeier, I. A. Zanoni, and L. A. Barton, *Proc. IEEE*, *56*, 1162 (1968).
58. W. Helfrich, *Mol. Cryst. Liq. Cryst.*, *21*, 187 (1973).
59. P. A. Penz, *Ibid.*, *15*, 141 (1971).
60. J. A. Castellano, *Ferroelectrics*, *3*, 29 (1971).

Received by editor December 9, 1974